2014 IEEE International Conference on Fuzzy Systems (FUZZ-IEEE)
July 6-11, 2014, Beijing, China

Fuzzy Proportional-Resonant Control Strategy for Three-Phase Inverters in Islanded Micro-Grid with Nonlinear Loads

Hongda Cai, Wei Wei, Yonggang Peng, and Huiyong Hu
College of electrical Engineering
Zhejiang University
Hangzhou, China
email: caihongda@zju.edu.cn, wwei@zju.edu.cn, pengyg@zju.edu.cn, huhuiyong@zju.edu.cn

***Abstract*—Conventional proportional-resonant controller is widely accepted and adopted in micro-grid applications. However, it's hard to design a satisfactory conventional proportion-resonant controller due to the contradictory nature of the inverter's stability, dynamic response speed and static tracking accuracy. Therefore, some trade-off strategies proposed in previous works are usually favored. This paper proposes a novel fuzzy proportional-resonant control strategy for a three-phase inverter, which can obtain better outcomes of three contradictory performance characteristics simultaneously. The detailed mathematical models and design procedure of the controller for the studied inverter are also presented. Compared with conventional proportional-resonant control strategy, the superiority of the proposed fuzzy proportional-resonant control strategy is significant for its better system stability, faster dynamic response speed and higher static tracking accuracy. Results from simulation are provided to verify the feasibility and effectiveness of the proposed approach.**

Keywords--Fuzzy proportional-resonant control; inverters; frequency-domain analysis; parameter design; nonlinear loads; power quality

I. INTRODUCTION

With the development of renewable energy sources and distribution generation, three-phase power electronic inverters have been widely used. On the basis of the characteristics of a micro-grid, scholars have proposed a variety of inverter control strategies[1]. However, most of them are based on a double loop control scheme which includes an inner current loop and an external voltage loop. However, the physical implementation becomes rather complex due to the synchronous rotating coordinate transformation.

Hence, an easy-to-implement conventional proportional-resonant (PR) control strategy with zero error tracking at fundamental frequency is proposed, which could handle with sinusoidal signals directly[2]. Nevertheless, the micro-grid is a system with strict requirements for the controllers' stability, dynamic capability and static tracking accuracy, which may make the conventional PR controllers still unsatisfactory in micro-grid applications.

In order to overcome the disadvantages of the conventional PR control strategy, this paper proposes a novel Fuzzy proportional-resonant(F-PR) control strategy, which is a sound solution for many existing problems in an islanded micro-grid such as the frequent load deviation, harmonic pollution from nonlinear loads, and the relatively poor stability. The proposed F-PR controller is a combination of a fuzzy logic controller and a conventional PR controller， and it can tune the PR gain parameters adaptively according to the expertise and fuzzy reasoning to make the inverter competent for various operating conditions. By improving the transient response speed of the inverter and enhancing the bus voltage quality, the inverters with F-PR control strategy are especially suitable for the sensitive loads which need a strictly standard voltage. The system configuration and design process of controllers are elaborated in section II and section III respectively. And then in Section IV, the comparison between the F-PR and the conventional PR controllers is made through simulation and the results verify the effectiveness and superiority of the proposed F-PR control strategy. Finally, conclusions are given in section V.

II. SYSTEM CONFIGURATION

The main circuit of a three-phase inverter used in an islanded micro-grid with both nonlinear loads and sensitive loads is shown in Fig.1, which needs a strict standard voltage to operate normally. The proposed system is composed of a DC source, a sinusoidal pulse-width modulation (SPWM) voltage source inverter (VSI), LC filters, and an isolation transformer between the inverter system and loads.

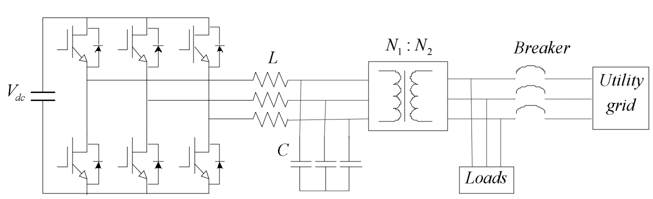

Fig.1. Configuration of the three-phase inverter system.

The rectifier type nonlinear loads would inject large amount of harmonic currents once they are connected to the micro-grid. The harmonic currents flow through the feeders will obviously degrade the voltage quality and have a huge

This work is supported by the National 863 Major Projects of China (2011AA050204), NSFC (61203299, 51377142), and the Fundamental Research Funds for the Central Universities of China (2013QNA4021) and the Zhejiang Province "Qiangjiang" Talents Program of China (2013R10047).

impact on the proper functioning of the sensitive loads. To improve the voltage quality and facilitate the normal operating of the sensitive loads, a fuzzy PR control strategy based on a conventional proportional-resonant controller is developed to regulate the inverter's output voltage that is applied on the sensitive loads.

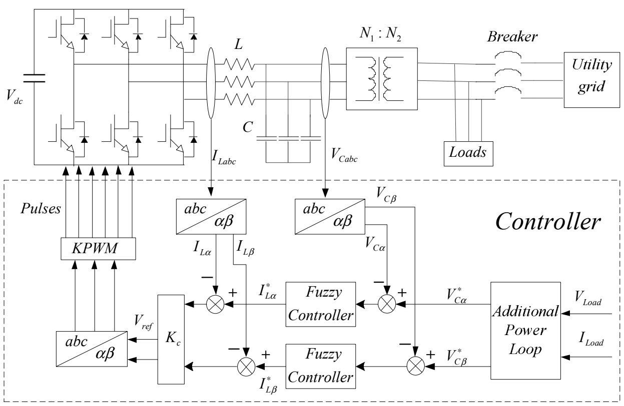

Fig.2. Power Circuit and control schematic for the three-phase inverter with LC filters.

As shown in Fig.2, the control scheme of the grid-interfacing inverter contains an internal current loop, an external voltage loop and an additional power control loop. The additional power control loop utilizes the conventional droop strategy to control the real power and reactive power to track the changes of the loads by varying the supply frequency and changing the voltage magnitude[3]. In order to overcome the disadvantages of the traditional proportional-resonant (PR) controller, a F-PR controller is applied in the external voltage loop. The voltage regulation loop uses three-phase load voltages as feedback variables so that zero tracking errors can be achieved. The inner current loop is implemented by using only proportional controllers $K_c$with three-phase inductor currents chosen as feedback variables, since it does not influence the tracking accuracy of the external voltage loop[4].

III. Controller Design

In this section, design of the fuzzy PR controller for the inverters to allow the islanded micro-grid in Fig.2 functioning as described in Section Ⅱ is demonstrated.(The design of fuzzy PR controller is based on that of conventional PR controller).

A. Conventional Proportional-resonant Controller Design

In [3], the authors introduced the power loop control scheme in detail, therefore it is not duplicated in this paper. Here attention is focused on the design of the outer voltage loop and inner current loop.

As shown in Fig.2, an outer capacitor voltage feedback regulator G_p is used to force the capacitor voltages$\{V_a, V_b, V_c\}$ to track their reference waveforms provided by the power loop stiffly with an acceptable low output total harmonic distortion (THD). The outputs of this voltage regulator $\{I^*_{La}, I^*_{Lb}, I^*_{Lc}\}$ are then fed to an inner inductor current controller K_c, acting as the inductor current reference signals. This inner current controller here is mainly to stabilize the system and to improve the system's dynamic response. The output modulating signals $\{m_a,\ m_b\ , m_c\}$ from the inner current loop are finally fed to the sinusoidal pulse-width modulator (SPWM) to generate the high frequency gating signals used for driving the three-phase VSI[5].

As illustrated in Fig.1, the circuit state equations of the three-phase SPWM inverter are as follows:

$$L\frac{di_L}{dt} = v_o - v_C \tag{1}$$

$$C\frac{dv_C}{dt} = i_L - i_{Load} \tag{2}$$

where L is the filter inductance, C is the filter capacitance, i_L and i_{Load} is the current flowing through the inductor and the loads, v_o is the voltage generated by the inverter and v_C is the filter capacitor voltage.

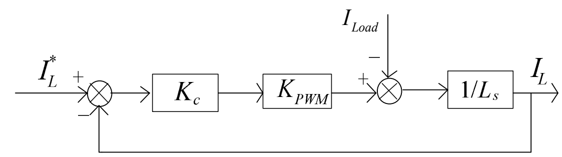

Fig.3. Block diagram of inner current loop.

The representation of (1) and (2) with inner inductor current control loop is shown in Fig.3, where the current of loads is represented as a disturbance input. Considering that $V_c = \left(I_L - I_{Load}\right)/Cs$, the following closed-loop transfer function for a single-phase equivalent model is obtained:

$$I_L = \frac{K_c K_{PWM} Cs}{LCs^2 + K_c K_{PWM} Cs + 1} I_L^* + \frac{1}{LCs^2 + K_c K_{PWM} Cs + 1}\ I_{Load} \tag{3}$$

Frequency domain analysis can now be performed using (3) to plot the Bode diagrams of $I_L/I_L^*$and I_L/I_{Load} as shown in Fig.4 and Fig.5 where $K_{PWM} = V_{dc}/2$ and $K_C = 1$.(The system parameters used are given in Table Ⅲ in section Ⅴ).

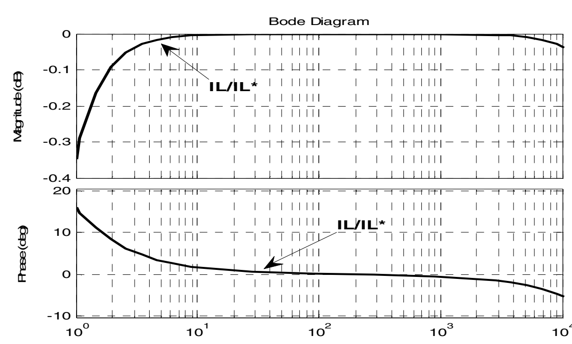

Fig.4. Bode plot of I_L/I_L^*.

Theoretically, the bandwidth of I_L/I_L^* in Fig.4 should be maximized by choosing a great gain of K_c. Obviously, a higher K_c will concentrate to achieving a zero error tracking to the reference I_L^* at all frequencies, a faster dynamic response and less disturbance generated from the changes of I_{Load} which means that I_L/I_{Load} will approach zero. However, an extremely large gain degrades the stability of the control system. Therefore, a proper K_c giving a near-zero closed-loop current gain at the fundamental frequency will be selected as a satisfactory compromise, which is 20 in this paper. Consequently, a closed-loop current gain I_L/I_L^* and a small I_L/I_{Load} gain are 0.0002 dB and -44.9024 dB respectively[6, 7].

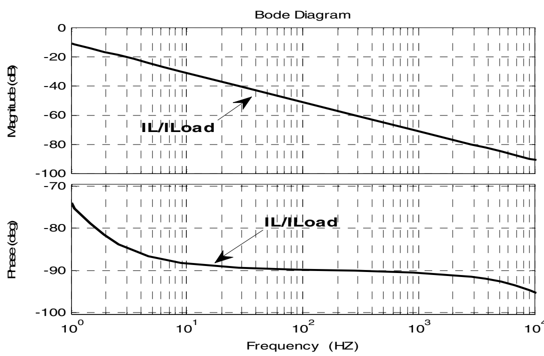

Fig.5. Bode plot of I_L/I_{Load}.

For the outer voltage loop, a proportional-resonant (PR) controller in stationary $\alpha-\beta$ frame is used due to its easier physical implementation and a theoretically infinite gain at the fundamental frequency, which will force the steady-state voltage errors to zero. Also, it is obvious that there is no cross coupling term in the $\alpha-\beta$ frame and the equations for the PR controller at fundamental frequency (50Hz) can be expressed as follows(where ω=314 *rad/s*):

$$G_p=K_p+\frac{K_r s}{s^2+\omega^2} \tag{4}$$

Where K_p and K_r are the coefficients.

The open-loop bode diagram is shown in Fig.6, which reveals the effects of K_r when K_p is set to a constant zero.

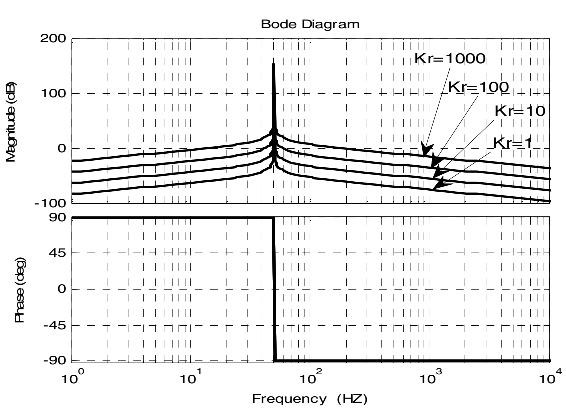

Fig.6. Bode plot of G_p.

According to Fig. 6, an infinite open-loop gain will be achieved at the frequency ω (Here 314 rad/sec), and the parameter K_r acts on the gain of the controller exclusively, so that the regulator can track sinusoidal reference signals at the fundamental frequency with zero error theoretically.

Once the inner current loop is determined and the modus of the outer voltage regulator is identified, the complete diagram of inner voltage and current loop is illustrated in Fig.7. With the specified voltage and current controllers, the closed-loop 'output voltage to reference' transfer function is derived as (5).

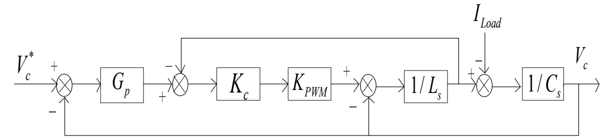

Fig.7. Block diagram of the inner voltage and current loops.

$$V_C=\frac{K_cK_{PWM}G_p}{LCs^2+K_cK_{PWM}Cs+G_pK_cK_{PWM}+1}V_C^* - \frac{K_cK_{PWM}+Ls}{LCs^2+K_cK_{PWM}Cs+G_pK_cK_{PWM}+1}I_{Load} \tag{5}$$

where $G_p=K_p+\frac{K_r s}{s^2+\omega^2}$ and the parameters are given in Table Ⅲ.

Similar to the inner inductor current loop, s-domain analysis can be executed and a satisfactory compromise of K_p and K_r between the attainable control bandwidth and the control loop stability is acquired. In this paper, K_p and K_r are chosen to give a steady-state voltage error of less than 1% at the fundamental frequency. Accordingly, K_p=2 and K_r=100 result in the closed-loop voltage response curve in Fig.8, which has a steady-state magnitude error of 0.02% and a phase error of 0.0000 ° at the fundamental frequency theoretically. As well, a negligibly small V_c/I_{Load} gain at the fundamental frequency can be seen in Fig. 8.

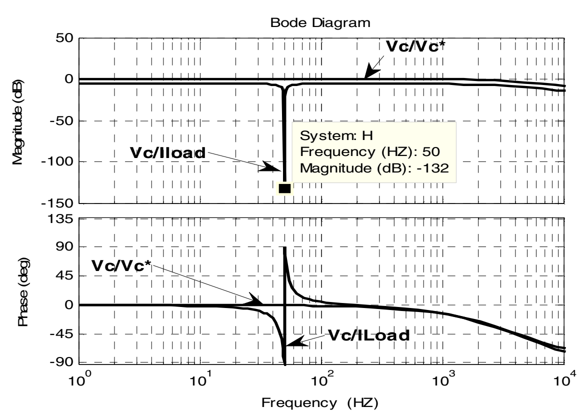

Fig.8. Bode plot of V_c/V_c^* and V_c/I_{Load}.

Using (5), the closed-loop transfer function from V_C^* *to* V_C without considering the influence of load disturbance is given by

$$G=\frac{K_c K_{PWM} G_p}{LCs^2+K_c K_{PWM} Cs+G_p K_c K_{PWM}+1} \tag{6}$$

Thereupon, the system's root locus for $K_p=0.01\rightarrow 10$ (when K_c and K_r are set as 20 and 100 respectively) is derived as in Fig.9.

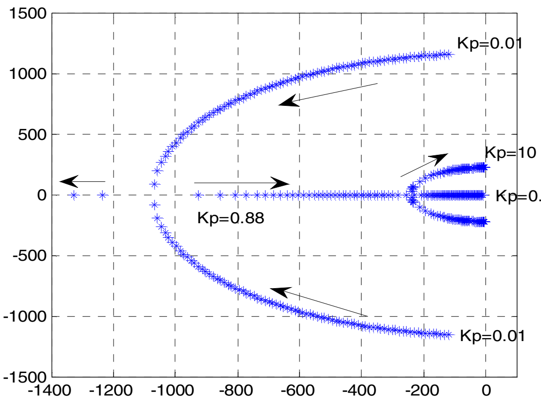

Fig.9. Root locus of the control system.

Fig.9 shows that the dominant poles will approach imaginary axis when the gain of K_p is set extremely large or small, which will degrade the system's stability margin. Therefore the gain of K_p should be a compromise between the stability and the speed of dynamic response. In summary, the gain parameters (K_c, K_p, and K_r) of the controllers chosen in this paper above are appropriate and efficient[7].

B. Fuzzy Proportional-resonant Controller Design

As described in the introduction, to overcome the disadvantages of the conventional proportional-resonant controller, the application of the Fuzzy Proportional-resonant (FPR) controller is proposed. The proposed Fuzzy-PR controller is a combination of PR controller and Fuzzy Logic Controller. The operation of the Fuzzy-PR controller is based on Fuzzy Logic Controller (FLC) for on–line tuning of the gains of the voltage PR regulator, K_p and K_r, as shown in (7) and (8). Then, the regulator uses the optimal adjusted gains K_p and K_r to get a better control performance, that means smaller static errors, faster dynamic response and better robustness[8].

$$K_p(n)=K_p(n\text{-}1)+\Delta K_p \tag{7}$$

$$K_r(n)=K_r(n\text{-}1)+\Delta K_r \tag{8}$$

The structure of the proposed F-PR controller is depicted in Fig.10. As inputs to the F-PR controller, the capacity voltage error e and the changes of error Δe are sampled. As outputs from the Fuzzy Logic Controller, the tuning parameters ΔK_p and ΔK_r are then fed to the PR regulators dynamically to adjust the controller to an optimal adaptive state. The scaling factors G_1, G_2, G_3, and G_4 are used to normalize the input and output signals[9, 10].

Fuzzification is the process of converting the accurate input signals into fuzzy values, where each accurate value is given a degree of membership to all the membership functions covering the universe discourse. Fuzzy inference engine concludes useful results from the fuzzified inputs based on the fuzzy rules in the rule-base, and then the fuzzy reasoning results are deffuzzified by the deffuzzifier with output membership functions[11].

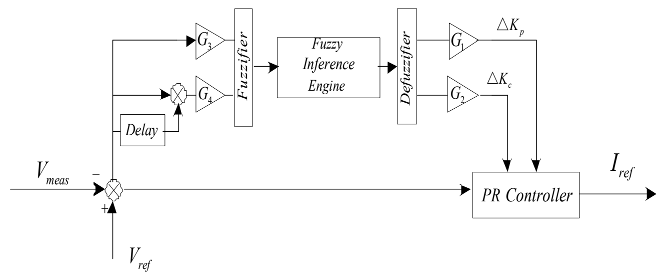

Fig.10. Structure of the Fuzzy PR controller.

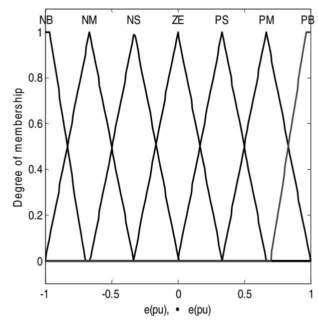

Fig.11. Membership functions for input variables.

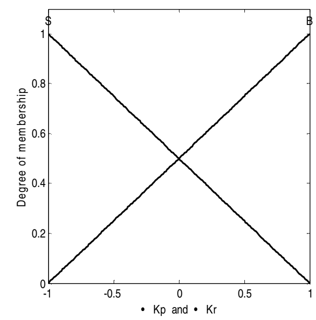

Fig.12. Membership functions for output variables.

In Fig.11, seven triangular membership functions are used for each input signal(note that NL represents for negative large, NM represents for negative medium, NS represents for negative small, ZE represents for zero, PS represents for positive small, PM represents for positive medium, PL represents for positive large). Fig.12 shows that only two membership functions are used for each fuzzy output results(B is for big and S is for small)[12]. These membership functions are chosen for their easy implement with favorable performance. In this F-PR controller the Mamdani inference method and the min-max composition are used, and the centroid method is used for the output membership function.

The greatest superiority of the F-PR controller is the on-line tuning of the gain parameters of the regulator, so that it can run in the optimal condition by the expertise. Once a step disturbance introduced by load switching occurs in the micro-grid bus voltage, we need a big control signal at the beginning to obtain a fast dynamic response[13-15]. Thus, the proportional and resonant gain's variation ΔK_p and ΔK_r can be represented by fuzzy set *Big*. With the degrading of e and Δe, the system will gradually stabilize and at this time we need to gradually decrease the output ΔK_p and ΔK_r till the system approaches a stable state to avoid a big overshoot and erratic elements. When the system becomes stable, a new relatively high open-loop gain K_p is needed to obtain less static errors and meanwhile, an extremely low resonant gain is advisable to improve the robustness and stability of the system[16]. The fuzzy rules are illustrated in Table Ⅰ (for ΔK_p) and Table Ⅱ (for ΔK_r). The adopted fuzzy rules are in the standard forms: IF e is A and Δe is B, Then ΔK_p is C and ΔK_r is D.

TABLE Ⅰ Fuzzy Control rules for ΔK_p

e / Δe	NL	NM	NS	ZE	PS	PM	PL
NL	B	B	B	B	B	B	B
NM	S	B	B	B	B	B	S
NS	S	S	B	B	B	S	S
ZE	S	S	S	B	S	S	S
PS	S	S	B	B	B	S	S
PM	S	B	B	B	B	B	S
PL	B	B	B	B	B	B	B

TABLE Ⅱ Fuzzy control rules for ΔK_r

e / Δe	NL	NM	NS	ZE	PS	PM	PL
NL	B	B	B	B	B	B	B
NM	B	S	S	S	S	S	B
NS	B	B	S	S	S	B	B
ZE	B	B	B	S	B	B	B
PS	B	B	S	S	S	B	B
PM	B	S	S	S	S	S	B
PL	B	B	B	B	B	B	B

For the PR parts in the F-PR controller, we use the same parameters selected in the design of the conventional PR controller.

IV. SIMULATION RESULTS

This section conducts a comparative study between the two controllers above. The circuit parameters of a three-phase inverter system is listed below.

TABLE Ⅲ System Parameters

Parameters	Values
System basic capacity	10kVA
Inverter switching frequency	10kHz
Inverter filter inductance	10mH
Inverter filter capacitance	80μF
DC-Link voltage	700V
AC-Bus voltage (line-line rms)	380V
Isolation transformer ratio	1:1
linear load 1	2.5kW
nonlinear load 2	7.5kW

Parameters K_p , K_r and K_c for the conventional PR controller designed by the frequency domain analysis in section Ⅲ are 2, 100, 20 respectively.

Parameters K_p, K_r and K_c for the fuzzy PR controller are designed identically to the conventional one so that to facilitate the comparison between them. The fuzzy domain for both inputs and outputs of the fuzzy logic controller are selected as [-1,1] as the shown in Fig.11 and Fig.12. The scaling factors G_1, G_2, G_3, and G_4 are 2.5, 300, 2, and 2 respectively and the membership functions and fuzzy control rules are designed as same as that in section Ⅲ part B.

Initially, the islanded $10KVA$ micro-grid system operates with linear $2.5KW$ loads and a $7.5\ KW$ rectify type nonlinear loads are connected at the time of 0.15s,. the total harmonic distortion(THD) of the output voltage and the dynamic response are chosen as the evaluation indicators.

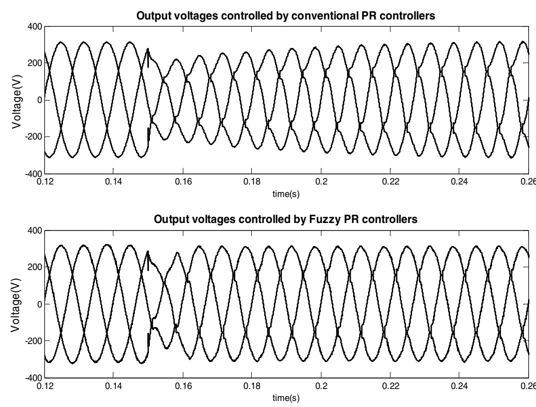

Fig.13. Output voltages controlled by the conventional PR controller and the Fuzzy PR controller respectively.

Fig.13 and Fig.14 show the comparison of three-phase voltage and current waveforms of inverters controlled by PR or F-PR controllers respectively. The fuzzy PR control strategy shows faster dynamic response about 0.08s (stabilize at 0.17s) than that of PR control strategy(stabilize at 0.25s) and better voltage waveforms while the currents' harmonic distortion are terribly serious as shown in Fig.14.

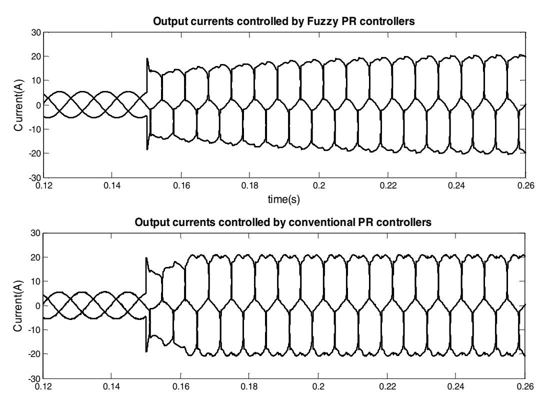

Fig.14. Output currents controlled by the conventional PR controller and the Fuzzy PR controller respectively.

The THD (total harmonic distortion) indexes under both F-PR and PR control strategies are shown in Fig.15 and obviously the F-PR control strategy can suppress the THD from 8.9% to 3.7% for supporting the sensitive load to run in a proper condition.

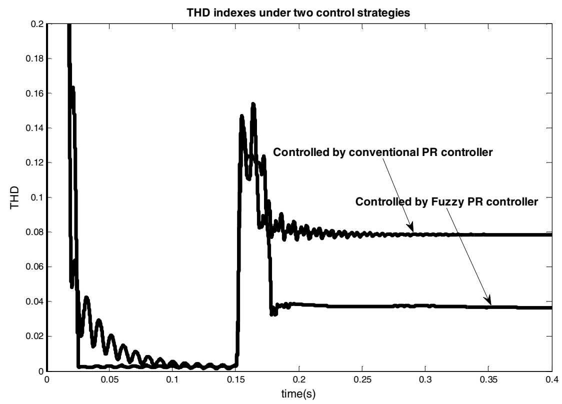

Fig.15. THD indexes comparison under the control of the two controllers.

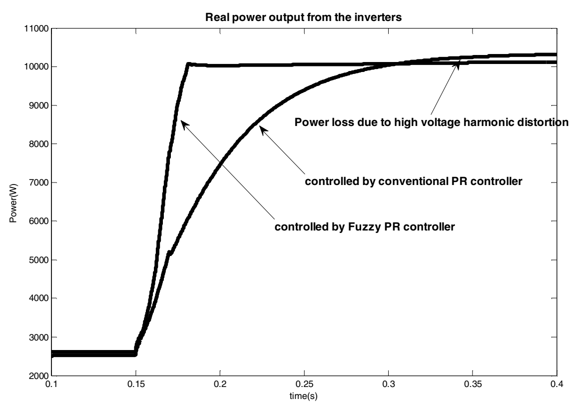

Fig.16. Comparison of output real power between inverters under two different control strategy.

The comparison of transient process of tracking the load changing of the two systems is shown in Fig.16. Just as discussed in section Ⅲ, the F-PR controller gives a more robust system with faster dynamic response.

V. CONCLUSION

This paper presents a novel Fuzzy proportional-resonant control strategy for three-phase inverters used in islanded micro-grid. The proposed control strategy employs a fuzzy logic controller combined with a proportional-resonant controller to tune the controller's gain parameters online, which can not only achieve faster dynamic response and higher static accuracy, but also suppress the voltage harmonics effectively. Simulation has confirmed the effectiveness and superiority of the proposed novel Fuzzy PR control strategy in comparison with the conventional PR control strategy.

REFERENCES

[1]. Lopes, J.P., C.L. Moreira and A.G. Madureira, Defining control strategies for microgrids islanded operation. *Power Systems, IEEE Transactions on*, 2006. 21(2): p. 916-924.

[2]. Zmood, D.N., D.G. Holmes and G.H. Bode, Frequency-domain analysis of three-phase linear current regulators. *Industry Applications, IEEE Transactions on*, 2001. 37(2): p. 601-610.

[3]. Yunwei, L., D.M. Vilathgamuwa and C.L. Poh, Design, analysis, and real-time testing of a controller for multibus microgrid system. *Power Electronics, IEEE Transactions on*, 2004. 19(5): p. 1195-1204.

[4]. Yun, W.L., D.M. Vilathgamuwa and C.L. Poh, A grid-interfacing power quality compensator for three-phase three-wire microgrid applications. *Power Electronics, IEEE Transactions on*, 2006. 21(4): p. 1021-1031.

[5]. Guerrero, J.M., et al., Advanced Control Architectures for Intelligent Microgrids—Part I: Decentralized and Hierarchical Control. *Industrial Electronics, IEEE Transactions on*, 2013. 60(4): p. 1254-1262.

[6]. Guan Y, Wu W, Guo X. Control Strategy for Three-phase Inverters Dominated Microgrid in Autonomous Operation[C]//Zhongguo Dianji Gongcheng Xuebao(Proceedings of the Chinese Society of Electrical Engineering). Chinese Society for Electrical Engineering, 2011, 31(33): 52-60.

[7]. Zhao Q, Guo X Q, Wu W. Research on control strategy for single-phase grid-connected inverter[C]//Zhongguo Dianji Gongcheng Xuebao(Proceedings of the Chinese Society of Electrical Engineering). 2007, 27(16): 60-64.

[8]. Wu D, Tan W W. Interval type-2 fuzzy PI controllers: Why they are more robust[C]//Granular Computing (GrC), 2010 IEEE International Conference on. IEEE, 2010: 802-807.

[9]. Khairy A, Ibrahim M, Abdel-Rahim N, et al. Comparing proportional-resonant and fuzzy-logic controllers for current controlled single-phase grid-connected PWM DC/AC inverters [C] // Renewable Power Generation (RPG 2011), IET Conference on. IET, 2011: 1-6.

[10]. Tsengenes G, Adamidis G. Comparative evaluation of Fuzzy-PI and PI control methods for a three phase grid connected inverter[C]//Power Electronics and Applications (EPE 2011), Proceedings of the 2011-14th European Conference on. IEEE, 2011: 1-10.

[11]. Huang Y, Yasunobu S. A general practical design method for fuzzy PID control from conventional PID control[C]//Fuzzy Systems, 2000. FUZZ IEEE 2000. The Ninth IEEE International Conference on. IEEE, 2000, 2: 969-972.

[12]. Mann, G.K.I., H. Bao-Gang and R.G. Gosine, Analysis of direct action fuzzy PID controller structures. *Systems, Man, and Cybernetics, Part B: Cybernetics, IEEE Transactions on*, 1999. 29(3): p. 371-388.

[13]. Zhao, Z., M. Tomizuka and S. Isaka, Fuzzy gain scheduling of PID controllers. *Systems, Man and Cybernetics, IEEE Transactions on*, 1993. 23(5): p. 1392-1398.

[14]. Jian L, Yong K, Jian C. Fuzzy-tuning PID control of an inverter with rectifier-type nonlinear loads[C]//Power Electronics and Motion Control Conference, 2000. Proceedings. IPEMC 2000. The Third International. IEEE, 2000, 1: 381-384.

[15]. Xiaojin Y, Jinhao S, Yezi L, et al. Self-adaptive tuning of fuzzy PID control of PV Grid-connected inverter[C]//Fuzzy Systems and Knowledge Discovery, 2009. FSKD'09. Sixth International Conference on. IEEE, 2009, 4: 160-162.

[16]. Wang Z, Ahn T. Design of the Optimal Self-tuning Fuzzy-PI Controller for Rectifier Current Control in HVDC System[C]//Control Conference, 2006. CCC 2006. Chinese. IEEE, 2006: 1224-1227.